

Dynamics of two air bubbles rising in a shear-thinning fluid

Purushotam Kumar*¹ and Surya P. Vanka†²

¹Corning Incorporated, Manufacturing Technology & Engineering, Corning, NY 14830

²Mechanical Science & Engineering, University of Illinois Urbana-Champaign, Urbana, IL 61801

January 18, 2023

Abstract

In this paper, we have studied the three-dimensional dynamics of two equally sized air bubbles rising in a shear-thinning fluid. We have used the combined level set and volume of fluid (CLSVOF) method to track interface, maintain mass balance and estimate the interface curvature. Additionally, we have incorporated a Sharp Surface Force Method (SSF) for surface tension forces. This method significantly suppressed the spurious velocities commonly observed with the conventional volume of fluid method and the Continuum Surface Force (CSF). The algorithm is implemented in an in-house code called CUFLOW and runs on multiple GPUs platform.

We have explored the effects of fluid rheology on the three-dimensional dynamics of two in-line bubbles. Two power-law indices (0.5 and 1) are investigated to highlight differences in shear-thinning and Newtonian fluids. For a range of parameters examined here, bubbles motion in a shear-thinning fluid is seen to be unsteady with significant shape oscillations. Further, we have examined the rise velocity, droplets rise path, transient shapes and found that modification of viscosity by the motion of the leading bubble changes the dynamics of the trailing bubble.

Keywords: Bubble dynamics; Bubble interactions; Liquid flow structure; Two-phase flows; Volume of fluid (VOF) method

1 Introduction

A gas bubble rising in a liquid medium is one of the simplest two-phase flow problems and addresses several important interactions between two phases. This problem has been previously studied to understand lift [Morsi and Alexander \(1972\)](#); [Kurose et al. \(2001\)](#) and drag [Magnaudet and Legendre \(1998\)](#) forces acting on a bubble, lateral migration of the bubble in a co-flow [Adoua et al. \(2009\)](#), and bubble-wall and bubble-wake interactions. A large number of researchers, including [Allen \(1900\)](#);

*pkumar8@illinois.edu

†spvanka@illinois.edu

Hadamard (1911); Rybczynski (1911); Bond (1927); Moore (1959) have investigated the bubble deformation, rise path, terminal velocity, and confinement effects through experiments, theoretical modeling, and numerical simulations.

Dynamics of a rising bubble are a function of the Eötvös number ($Eo = \Delta\rho gd^2\sigma^{-1}$, also referred as Bond number $Bo = \rho_lgd^2\sigma^{-1}$), Morton number ($Mo = g\mu_o^4\rho_l^{-1}\sigma^{-3}$), confinement ratio ($C_r = Wd^{-1}$), and other external forces such as a magnetic field ? and variable viscosity Kumar et al. (2015a). An exhaustive collection of experimental data for a bubble rising in an unconfined medium has been summarized in works of Grace (1973); Grace et al. (1976); Bhaga and Weber (1981), available as nomogram charts of the terminal Reynolds and bubble shape for combinations of Bond and Morton numbers. In addition, the proximity of the bubble to a wall alters the bubble rise velocity and shape and increases the shear force at the gas-liquid interface Figueroa-Espinoza et al. (2008); Kumar and Vanka (2015). Detailed reviews of bubble dynamics in Newtonian fluids are available in the works of Clift et al. (1978); DeKee (2002).

The dynamics of bubbles in Newtonian fluids have been widely studied. However, many fluids have non-Newtonian behavior and are used in the chemical and pharmaceutical industries. For instance, the fermentation of liquor, sugarcane processing, ethanol extraction, aeration of the membrane is typical shear-thinning applications. Bubble rise in non-Newtonian fluids is more complex because the bubble-generated velocities subsequently change the local fluid viscosity due to the shear. Further, the nature of the fluid (Bingham, thixotropic, shear-thinning, shear-thickening, etc.) is important in modifying the fluid viscosity in the bubble vicinity and thereby the local shear stress values. Thus, a large parameter space is available, even for a single bubble in a non-Newtonian fluid, which provides rich and complex flow physics regions. Previously, several efforts have been made towards understanding such bubble motion in viscoelastic and inelastic non-Newtonian fluids. Some example works are by Astarita and Apuzzo (1965); Leal et al. (1971); Carreau et al. (1974); Zana and Leal (1978); Kawase and Ulbrecht (1981); Dekée et al. (1986); Gummalam et al. (1988); Kee et al. (1990); Manjunath and Chhabra (1992); Miyahara and Yamanaka (1993); Liu et al. (1995); Rodrigue et al. (1996); Li et al. (1997); Chhabra (1998); Gauri and Koelling (1998); Dubash and Frigaard (2007); Tsamopoulos et al. (2008); Sikorski et al. (2009); Kishore et al. (2013); Tripathi et al. (2015) for bubble motion in shear-thinning, shear-thickening and Bingham fluids. The papers of Kulkarni and Joshi (2005); Chhabra (2006) provide good summaries of the important results.

The dynamics of multiple bubbles rising has been studied by several authors (Abbassi et al., 2018; Gumulya et al., 2017; Watanabe and Sanada, 2006; Yuan and Prosperetti, 1994; Legendre et al., 2003; Yu et al., 2011; Katz and Meneveau, 1996; Ruzicka, 2000) and have reported that flow structure around the bubble has an important impact on the interaction between leading and trailing bubbles. They have reported that wake in front of a trailing bubble plays an important role in reducing the drag around it. Due to reduced drag, the trailing bubble accelerates until it coalesces with the

leading bubble. Along with these, there are other studies; however, the majority of the studies for multiple bubble rise are conducted in the Newtonian fluids.

In the present paper, we have briefly discussed a numerical technique to simulate two-phase flows and used it to study the three-dimensional deformation and rise of two equally sized bubbles in shear-thinning and Newtonian fluids for a given bubble size and center to center distance. Despite a reasonably large number of previous studies, there are very few studies that have examined the dynamics of in-line bubbles rising in non-Newtonian fluids. Various quantities such as the bubble shape, rise velocity, and rise paths are investigated. The algorithm used for the computations is presented in the numerical method section. The problem description is provided in the computational details section 3. In the results and discussion section 4, we present the results of the simulations and discuss the critical findings. A summary of the present findings is given at the end.

2 Numerical Method

We have developed a numerical procedure that solves the relevant governing equations on a fixed Eulerian collocated grid. The procedure consists of algorithms for interface capturing, the inclusion of surface tension forces, and the solution of Navier-Stokes equations. The volume of fluid (VOF) method of Hirt and Nichols [Hirt and Nichols \(1981\)](#) is used for interface capturing. The truncated interface between the gas and liquid in a control volume is represented as an oblique plane, and the interface normal, and curvature are computed using a smoothed liquid volume fraction and the height function method ([Rudman \(1998\)](#) and [Cummins et al. \(2005\)](#)), respectively. We have incorporated the surface tension force in Navier-Stokes equations using a sharp surface force (SSF) and pressure balance methods ([Francois et al. \(2006\)](#), [Wang and Tong \(2010\)](#)). The Navier-Stokes equations are solved using the fractional step method. The numerical procedure has been previously used to study the effects of duct confinement on dynamics of bubble rising in a square duct [Kumar and Vanka \(2015\)](#); [Kumar et al. \(2015b\)](#) and the effects of magnetic field on bubble dynamics [Jin et al. \(2016\)](#).

Governing Equations

We assume that both the gas and liquid are isothermal and incompressible. A single fluid approach with a method to capture the interface between gas and liquid is used. The combined governing equations for both fluids are given by the following equations:

$$\nabla \cdot \mathbf{u} = 0 \tag{1}$$

$$\begin{aligned} \frac{\partial(\rho\mathbf{u})}{\partial t} + \nabla \cdot (\rho\mathbf{u}\mathbf{u}) = & -\nabla p + \nabla \cdot (\mu [\nabla\mathbf{u} + \nabla\mathbf{u}^T]) \\ & + \rho\mathbf{g} + \sigma\kappa\mathbf{n}\delta(\mathbf{x} - \mathbf{x}_f) \end{aligned} \quad (2)$$

In the above equations, \mathbf{u} is the fluid velocity, p is pressure, ρ is density, μ is dynamic viscosity, σ is surface tension coefficient, κ is interface curvature, \mathbf{n} is interface normal, δ is the delta function, \mathbf{x} is the spatial location where the equation is solved, \mathbf{x}_f is the position of the interface and \mathbf{g} is the acceleration due to gravity.

Since the free surface is captured by the volume of fluid method, a time evolution of VOF function (liquid volume fraction, α) given by

$$\frac{\partial\alpha}{\partial t} + \mathbf{u} \cdot \nabla\alpha = 0 \quad (3)$$

is solved. The geometry construction method (Rider and Kothe [Rider and Kothe \(1998\)](#)) coupled with a second-order operator split method (Noh and Woodward [Noh and Woodward \(1976\)](#), Li [Li \(1995\)](#), Ashgriz and Poo [Ashgriz and Poo \(1991\)](#) and Francois et al. [Francois et al. \(2006\)](#)) is used to solve the evolution equation. The mixture density and viscosity are calculated as a linear weighting of the individual phase values, as

$$\rho = \alpha\rho_l + (1 - \alpha)\rho_g \quad (4)$$

$$\mu = \alpha\mu_l + (1 - \alpha)\mu_g \quad (5)$$

The subscripts l and g denote gas and liquid phases, respectively. The last term in eq. (2) is the surface tension force, and $\sigma\kappa$ is the pressure jump at the free surface. In our current algorithm, the jump condition is enforced explicitly by representing the surface tension force as a pressure gradient given by

$$\sigma\kappa\mathbf{n}\delta(\mathbf{x} - \mathbf{x}_f) = -\nabla\tilde{p} \quad (6)$$

Where \tilde{p} is the pressure solely due to the surface tension force at the interface. An elliptic equation for \tilde{p} is derived from continuity and momentum equations,

$$\nabla \cdot \left(\frac{\nabla\tilde{p}}{\rho} \right) = 0 \quad (7)$$

The jump condition at the interface is enforced by using eq. (6) as a source term in the solution of eq. (7). This ensures the exact difference in pressure at the interface due to the surface tension. In our work, this elliptic equation for \tilde{p} is efficiently solved using a multigrid accelerated red-black SOR relaxation scheme implemented on a GPU. Using this method, the spurious velocities reduces

to machine zero for a static bubble with exact analytical curvature and to very small values when the curvature is numerically computed. Admittedly, there are several methods to include the surface tension force in the Navier-stokes (Renardy and Renardy [Renardy and Renardy \(2002\)](#), Sussman et al. [Sussman \(2003\)](#); [Sussman et al. \(2007\)](#), Gueyffier et al. [Gueyffier et al. \(1999\)](#)); however, in our experience, the current method is more accurate for reduction of spurious velocities and relatively easier to implement on GPUs.

Solution Procedure

The following steps outline solution of the governing equations,

1. Initialize the solution with initial liquid fraction (α^n) and velocities (\mathbf{u}^n)
2. Calculate the density and viscosity at n^{th} time step using,

$$\begin{aligned}\rho^n &= \alpha^n \rho_l + (1 - \alpha^n) \rho_g \\ \mu^n &= \alpha^n \mu_l + (1 - \alpha^n) \mu_g\end{aligned}$$

3. Solve the interface tracking equation (using \mathbf{u}^n) to obtain α^{n+1}
4. Calculate the density (ρ^{n+1}) and viscosity (μ^{n+1}) using α^{n+1}
5. Calculate the interface curvature using the height function method
6. Solve the pressure (\tilde{p}) using sharp surface force method

$$\nabla \cdot \left(\frac{\nabla \tilde{p}}{\rho} \right)^{n+1} \quad \text{with } \nabla \tilde{p} = -(\sigma \kappa \mathbf{n} \delta(\mathbf{x} - \mathbf{x}_f))^{n+1}$$

7. Compute the pressure gradient term $\left(\frac{\nabla \tilde{p}}{\rho} \right)^{n+1}$ at cell faces
8. Compute the convection term $(\nabla \cdot \rho \mathbf{u} \mathbf{u})$ using geometry construction method
9. Compute the intermediate velocities at cell centers as,

$$\begin{aligned}\rho_c^{n+1} \hat{\mathbf{u}}_c &= \rho_c^n \mathbf{u}_c^n - \Delta t \sum_f \mathbf{u}_c^n \left(\sum_{k=1}^2 \rho_k^n \alpha_k^n \right) A_f \\ &\quad + \Delta t \sum_f \mu_f^n (\nabla \mathbf{u}^n + \nabla^T \mathbf{u}^n)_f \cdot \mathbf{n}_f + \rho_c^{n+1} \left(\frac{\nabla \tilde{p}}{\rho} \right)_{f \rightarrow c}^{n+1}\end{aligned}$$

10. Compute the intermediate velocities at cell faces as,

$$\hat{\mathbf{u}}_f = \hat{\mathbf{u}}_{c \rightarrow f}$$

11. Compute pressure (p) using,

$$\nabla \cdot \left(\frac{\nabla p}{\rho} \right)^{n+1} = \frac{\nabla \cdot \hat{\mathbf{u}}_f}{\Delta t}$$

12. Correct the velocity field for divergence free condition using,

$$\mathbf{u}_c^{n+1} = \hat{\mathbf{u}}_c - \Delta t \left(\frac{\nabla p}{\rho} + \frac{\nabla \tilde{p}}{\rho} \right)_{f \rightarrow c}^{n+1}$$

Where, $c \rightarrow f$ represents the linear averaging procedure to compute face value (eg. $\rho_f, \mu_f, \mathbf{u}_f$) from its cell-centered values. The intricate details of the numerical algorithm are described in Kumar and Vanka [Kumar and Vanka \(2015\)](#).

The entire algorithm has been programmed on the CUDA-Fortran platform supported by the Portland Group (PGI) Fortran compiler to run on multiple graphics processing units (GPU). Previously, we have validated the multiple GPU implementation ([Kumar et al., 2015b](#); [Vanka et al., 2016](#); [Kumar, 2016](#)) to study confinement effects on bubble dynamics ([Kumar and Vanka, 2015](#)), two-phase flows at T-junctions ([Horwitz et al., 2012, 2013](#); [Kumar et al., 2013](#)), bubble dynamics in non-Newtonian fluids ([Kumar et al., 2015a, 2019](#)), droplet dynamics in square duct ([Horwitz et al., 2014, 2019](#)), Argon bubble rising in liquid steel ([Vanka et al., 2015](#); [Jin et al., 2016](#); [Kumar and Vanka, 2022](#); [Kumar and Vanka, 2023](#)) and turbulent bubbly flow ([Vanka et al., 2016](#); [Kumar and Vanka, 2021](#)).

3 Computational Details

Problem Setup

Figure 1 shows the geometry of the problem considered. The dimensions of domain are $4d \times 4d \times 24d$ along x, y and z directions respectively. The height was chosen such that the bubble in a Newtonian fluid can reach a steady velocity at the end of the domain. All boundaries of the domain are considered to be no-slip and no-penetration walls. The trailing bubble is initially placed two diameters above the bottom boundary in the center of the duct cross-section. The leading bubble is placed according to the bubble's center to center distance of the problem (in this case $4d$). The gravitational force acts downwards along the negative z -axis. Based on a systematic grid refinement study, we have selected 32 control volumes per bubble diameter as an adequate resolution, with a grid of $128 \times 128 \times 768$ (≈ 13 million) control volumes current study.

The liquid and gas densities are taken as 1000 and 1.2 kg/m^3 . The zero shear viscosity (μ_0) and time constant (λ) of the liquid are 0.014 Pa.s and 1 s respectively. The power-law index is varied from each case. The dynamic viscosity of the gas (μ_g) is taken as $1.8 \times 10^{-5} \text{ Pa.s}$. The surface

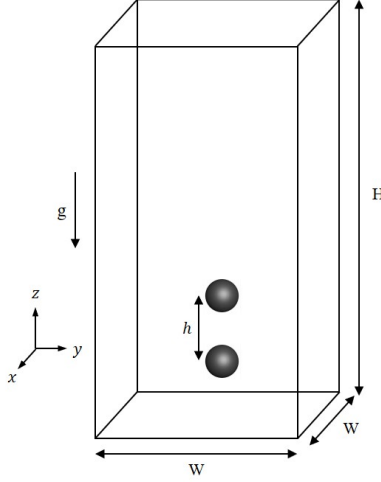


Fig. 1: Initial position of the bubble

tension (σ) between liquid and gas phase is prescribed a value of $0.072N/m^1$.

The liquid viscosity is calculated using the Carreau model [Carreau \(1972\)](#) with the power-law index 0.5 and 1.0 for shear-thinning and constant viscosity, respectively. It is calculated using,

$$\mu_l(\dot{\gamma}) = \mu_o(1 + (\lambda\dot{\gamma})^2)^{n-1/2} \quad (8)$$

Where, μ_o , λ and n are zero shear viscosity, time constant and power-law index, respectively. The shear rate ($\dot{\gamma}$) is given as,

$$\dot{\gamma} = \sqrt{2\mathbf{D} : \mathbf{D}} \quad (9)$$

The deformation tensor \mathbf{D} is defined as,

$$\mathbf{D} = 1/2 (\nabla\mathbf{u} + \nabla\mathbf{u}^T) \quad (10)$$

¹In practice there is variation in the surface tension due to addition of polymers for preparation of shear-thinning and shear-thickening fluids but the variation is relatively less significant for low concentration of polymers [Ohta et al. \(2003\)](#); [Zhang et al. \(2010\)](#); [Ohta et al. \(2012\)](#)

The dynamics of two bubbles ascending are governed by four non-dimensional parameters,

$$\text{Eötvös number} = Eo = \frac{\Delta\rho g d^2}{\sigma} \quad (11)$$

$$\text{Morton number} = Mo = \frac{g\mu_l^4 \Delta\rho}{\rho_l^2 \sigma^3} \quad (12)$$

$$\text{Confinement ratio} = Cr = \frac{W}{d} \quad (13)$$

$$\text{center to center distance} = h_d = \frac{h}{d} \quad (14)$$

In the above equations, $\Delta\rho = \rho_l - \rho_g$, W is width of liquid column and h is the initial center to center distance of bubbles. For a gas-liquid system the density ratio is large, hence $\Delta\rho = \rho_l - \rho_g \approx \rho_l$ and Eötvös number can be also represented by Bond number. In the current study, the viscosity of the liquid phase (μ_l) varies with the shear rate ($\dot{\gamma}$), therefore we define the Morton number using the zero-shear liquid viscosity. Hence, the key non-dimensional parameters are given by:

$$\text{Bond number} = Bo = \frac{\rho_l g d^2}{\sigma} \quad (15)$$

$$\text{Morton number} = Mo = \frac{g\mu_{l,0}^4}{\rho_l \sigma^3} \quad (16)$$

$$\text{Confinement ratio} = Cr = \frac{W}{d} \quad (17)$$

$$\text{center to center distance} = h_d = \frac{h}{d} \quad (18)$$

4 Results and Discussion

We now present the results of a study to analyze the effects of fluid rheology on bubble deformation, rise velocity, rise path, and liquid viscosity distribution. Two power-law indices (0.5 and 1.0) have been considered to understand its effects. The power-law indices capture the shear-thinning and Newtonian behavior of the non-Newtonian fluid. The zero-shear viscosity (μ_0) and time constant (λ) of the Carreau model [Carreau \(1972\)](#) have been kept constant to isolate the effects of the power-law index. The bubbles are initially placed at the center of the cross-section, but the bubbles may come closer to the wall during the ascend. The Bond is kept constant at $Bo = 2$, and the terminal shape in the Newtonian fluid is expected to be ellipsoidal.

Now, we discuss the effects of the power-law index (n) for a center to center distance of $4d$. For two liquids considered here, the zero-shear Morton number (Mo) is 10^{-6} . According to the Grace diagram [Grace \(1973\)](#), an initially spherical bubble of $Bo = 2$ rising in a Newtonian fluid with a Morton number of 10^{-6} deforms into an ellipsoidal shape. In non-Newtonian fluids, the viscosity will be modified by the shear generated adjacent to the bubble. Hence, the effective viscosity will

be lower for the shear-thinning fluid. Consequently, the effective Morton number of shear-thinning fluid will be lower than that of the Newtonian fluid.

		time (ms)				
n		0	80	160	240	320
0.5	LB					
0.5	TB					
1.0	LB					
1.0	TB					

Fig. 2: Transient three-dimensional front views of the bubbles for center to center distance = $4d$, and two power-law indices (n)

Figure 2 shows the transient shapes of leading (LB) and trailing (TB) bubbles for $n = 0.5$ and 1 and $h_d = 4$. From fig. 2 we can observe that the bubble terminal shape in the Newtonian fluid (Fig. 2 row 3) is ellipsoidal with nearly symmetrical top and bottom surfaces. However, in the shear-thinning fluid (Fig. 2 row 1), the bubble deforms into an ellipsoid that is flatter than its Newtonian counterpart with definite asymmetry between top and bottom surfaces. It can also be noticed that the bubble in shear-thinning fluid goes through shape and orientation oscillations. In contrast, in the Newtonian fluid, the bubble achieves a steady shape and rises without any orientation changes.

For the simulation time considered in this study, the dynamics of leading and trailing bubbles are quite similar in a Newtonian fluid. On the other hand, in shear-thinning fluid, their dynamics are complex. At $t = 80 \text{ ms}$, the shape of both bubbles is nearly identical, primarily because the trailing bubble has not yet reached the flow field modified by the leading bubble. The orientation and shape of the leading and trailing bubbles are different afterward. At $t = 160 \text{ ms}$, the surface normal at the top is upward-front and upward-back orientated for leading and trailing bubbles, respectively. This indicates that vortex shedding behind the bubble is oriented differently. At $t = 320 \text{ ms}$, the shape of the trailing bubble is upside-down of the leading bubble.

Figure 3 shows the ascending path of leading and trailing bubbles for a center to center distance of $4d$ and two power-law indices. It can be noticed that bubbles in the Newtonian fluid rise in a rectilinear path. This is in line with our observation from Fig. 2, the bubble reached a steady shape without any shape or orientation oscillations. It has also been reported earlier by Kumar et al. [??] that in the absence of bubble shape or orientation oscillations, the vortices behind the bubble are symmetric and do not amplify any instability. We are also observing similar phenomena for both

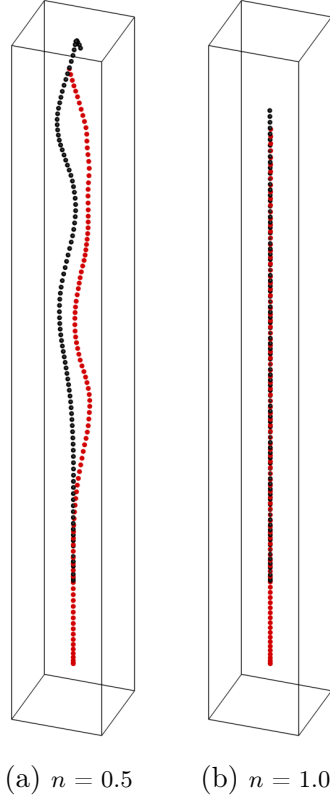


Fig. 3: Bubble rise path for center to center distance = $4d$, and two power-law indices

bubbles in the Newtonian fluid.

In the shear-thinning fluid, the rise path of bubbles goes from rectilinear to oscillatory. It should be noted that initially the trailing bubble has a smaller velocity and is away from the flow field modified by the leading bubble. Its shape changes from the spherical to asymmetric ellipsoid and doesn't exhibit surface oscillations. This is the primary reason for the initial rectilinear path of the bubble. As the bubble accelerates, it reaches a certain critical speed (or Reynold number), after which it sheds asymmetric vortices. This leads to non-uniform pressure distribution behind the bubble, which pushes the bubble away from the center of the liquid column and creates a zig-zag rise path. From Fig. 3(a) we can observe that the leading bubble initially migrates towards the left compared to the trailing bubble migrating towards the right.

Figure 4 shows the rise velocities of leading and trailing bubbles in the Newtonian and shear-thinning fluids for a center to center distance of 4. In the Newtonian fluid, the velocity curves of both bubbles are identical for up to $t \approx 60$ ms, and afterward, the curves diverge. The velocity of the leading bubble between 60 ms and 200 ms is almost constant, whereas the trailing bubble rapidly accelerates to achieve a higher velocity than the leading bubble. This behavior is primarily because the leading bubble ascends through the undisturbed flow field hence experiences maximum

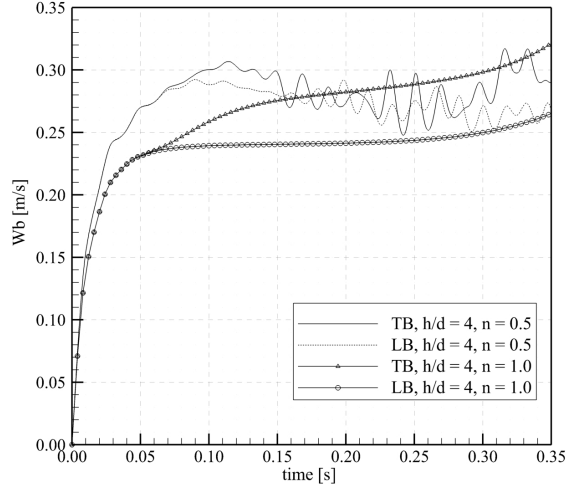


Fig. 4: Rise velocity of bubbles for center to center distance = $4d$, and two power-law indices

drag. The trailing bubble ascends through a modified flow field; as a result, it experiences lower drag force and achieves higher rise velocity.

Similar to the Newtonian case, rise velocity curves in the shear-thinning fluid are identical for up to $t \approx 70 \text{ ms}$, and afterward, the curves diverge. The rise velocity goes through rapid oscillations. In the Newtonian fluid, the trailing bubble velocity was always higher than that of the leading bubble. However, in the shear-thinning fluid, there are instances where the leading bubble rises with higher velocity than the trailing bubble. It can be noted for any given time window, the amplitude of oscillation of trailing bubble rise velocity is higher than that of the leading bubble.

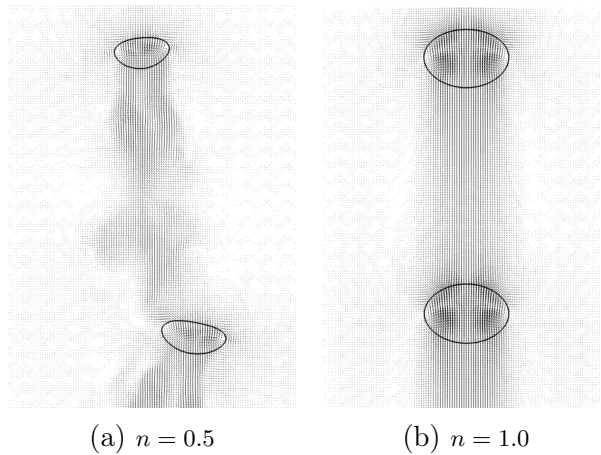


Fig. 5: Velocity vector at $t = 160 \text{ ms}$ for center to center distance = $4d$, and two power-law indices

Figures 5(a) and 5(b) show the velocity vectors on yz -plane at $t = 160 \text{ ms}$ for shear-thinning and constant viscosity cases. The interface has been drawn to show the cross-section of the bubble on

the yz - plane. We notice from Fig. 5(b) that velocity vectors in front of the trailing bubble are streamlined without any recirculation zones, and on both left and right sides, the flow distribution is symmetric. From Fig. 5(a) we can notice that the flow field in front of the trailing bubble contains recirculation zones and is asymmetric on the left and right sides of the bubble. The interaction between the recirculation zone and bubble creates asymmetric forces and pushes away from the centerline. The impact of this was observed in Fig. 3(a).

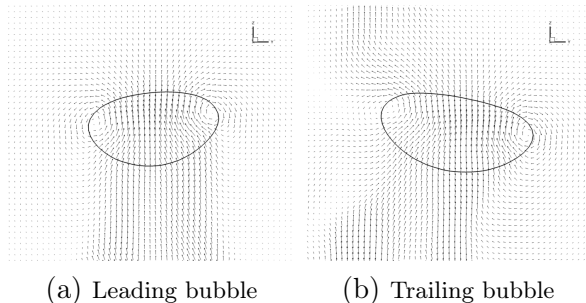


Fig. 6: Velocity vector at $t = 160 \text{ ms}$ for center to center distance = $4d$, and two power-law index = 0.5

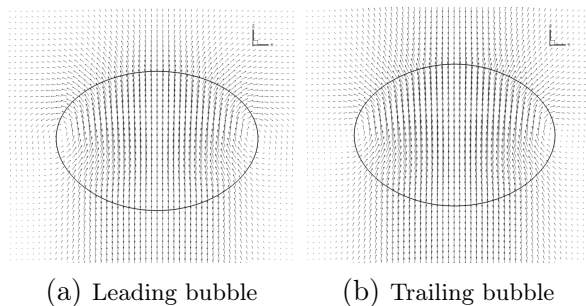


Fig. 7: Velocity vector at $t = 160 \text{ ms}$ for center to center distance = $4d$, and two power-law index = 1.0

Figures 6 and 7 show the zoomed-in view of bubbles at $t = 160 \text{ ms}$ on the yz -plane. The zoom ratio of the four subfigures is kept the same to show that the deformation of the bubble in the shear-thinning fluid is substantially higher than that in the Newtonian fluid. We can further observe the asymmetric and symmetric flow field around the trailing bubbles in shear-thinning and Newtonian fluid, respectively.

5 Conclusions

In this numerical study, we have compared the effects of fluid rheology on the three-dimensional dynamics of two in-line bubbles rising in a quiescent liquid medium. We have used a volume of fluid method coupled with a three-dimensional geometry construction method for accurate representation and advection of the interface. We have modeled the surface tension using the sharp surface force (SSF) method. The fractional step method with the implicit treatment of the viscous terms and

geometry construction method for the convection term has been used to solve the Navier-Stokes equations. The effects of the power-law index on the bubble shapes, rise velocity, rise path, and flow field at representative times have been explored.

We observe that the bubble deformation is strongly dependent on the power-law index of the fluid – in the Newtonian fluid, both leading and trailing bubbles deformed into an ellipsoid with symmetric top and bottom surfaces and attained steady-state shape. In contrast, the bubble became more flatter with asymmetric top and bottom surfaces in the shear-thinning fluid and went through surface oscillations as they ascended.

Further, we observe that the bubbles initially rose in a linear path in shear-thinning fluid and later followed a zigzag path. In contrast, in the Newtonian fluid, they rose in a rectilinear path throughout the ascent. The zigzag motion of the leading bubble was triggered by an asymmetry in the flow field behind and consequent vortex shedding behind the bubble. The zigzag motion of the trailing bubble is the combination of the unsteady flow in front of it and the asymmetric flow around it.

The rise velocity oscillates in the shear-thinning fluids, whereas no such features are present in the Newtonian and shear-thickening fluids. These oscillations are related to the shape oscillation of the bubble and a zigzag rise path. In both liquids, leading and trailing bubbles initially ascended with identical speeds. Once they achieved maximum deformation, the trailing bubble in the Newtonian fluid rose faster than the leading bubble. In the shear-thinning fluid, the magnitude of oscillation of rising velocity was higher for the trailing bubble than the leading bubble.

References

- S. A. Morsi and A. J. Alexander. An investigation of particle trajectories in two-phase flow systems. *Journal of Fluid Mechanics*, 55:193–208, 9 1972. ISSN 1469-7645. doi: 10.1017/S0022112072001806.
- R. Kurose, R. Misumi, and S. Komori. Drag and lift forces acting on a spherical bubble in a linear shear flow. *International Journal of Multiphase Flow*, 27(7):1247 – 1258, 2001. ISSN 0301-9322. doi: [http://dx.doi.org/10.1016/S0301-9322\(00\)00073-2](http://dx.doi.org/10.1016/S0301-9322(00)00073-2).
- Jacques Magnaudet and Dominique Legendre. The viscous drag force on a spherical bubble with a time-dependent radius. *Physics of Fluids*, 10(3), 1998.
- Richard Adoua, Dominique Legendre, and Jacques Magnaudet. Reversal of the lift force on an oblate bubble in a weakly viscous linear shear flow. *Journal of Fluid Mechanics*, 628:23–41, 6 2009. ISSN 1469-7645. doi: 10.1017/S0022112009006090. URL http://journals.cambridge.org/article_S0022112009006090.

- H. S. Allen. The motion of a sphere in a viscous fluid. *Philosophical Magazine Series 5*, 50(304): 323–338, 1900.
- J. Hadamard. Mouvement permanent lent d'une sphere liquide et visqueuse dans une liquide visqueux. *Comptes rendus de l'Académie des sciences*, 152:1735, 1911.
- W. Rybczynski. On the translatory motion of a fluid sphere in a viscous medium. *Bull. Acad. Sci., Krakow, Series A*, 40:40–46, 1911.
- W.N. Bond. Bubbles and drops and Stokes' law. *Philosophical Magazine Series 7*, 4(24):889–898, 1927.
- D. W. Moore. The rise of a gas bubble in a viscous liquid. *Journal of Fluid Mechanics*, 6(01): 113–130, March 1959. ISSN 0022-1120.
- Purushotam Kumar, Kai Jin, and S. Pratap Vanka. Bubble rise and deformation in a non-newtonian fluid in a square duct. *Computational Methods and Tools in Thermal Fluids Sciences*, pages 1–15, 2015a.
- JR Grace. Shapes and velocities of bubbles rising in infinite liquids. *Trans. Inst. Chem. Eng.*, 51 (2):116–120, 1973.
- J.R. Grace, T. Wairegi, and T.H Nguyen. Shapes and velocities of single drops and bubbles moving freely through immiscible liquids. *Chemical Engineering Research and Design*, 54a:167–173, 1976.
- Dahya Bhaga and M.E. Weber. Bubbles in viscous liquids: shapes, wakes and velocities. *Journal of Fluid Mechanics*, 105:61–85, 1981.
- B. Figueroa-Espinoza, R. Zenit, and D. Legendre. The effect of confinement on the motion of a single clean bubble. *Journal of Fluid Mechanics*, 616:419–443, November 2008. ISSN 0022-1120.
- P. Kumar and S.P. Vanka. Effects of confinement on bubble dynamics in a square duct. *International Journal of Multiphase Flow*, 77:32 – 47, 2015. ISSN 0301-9322.
- Roland Clift, John R Grace, and Martin E Weber. *Bubbles, Drops and Particles*. Academic Press, London, 1978.
- Daniel DeKee. *Transport Processes in Bubbles, Drops and Particles*. CRC Press, 2002.
- Gianni Astarita and Gennaro Apuzzo. Motion of gas bubbles in non-newtonian liquids. *AIChE Journal*, 11(5):815–820, 1965. ISSN 1547-5905. doi: 10.1002/aic.690110514. URL <http://dx.doi.org/10.1002/aic.690110514>.

- L. G. Leal, J. Skoog, and A. Acrivos. On the motion of gas bubbles in a viscoelastic liquid. *The Canadian Journal of Chemical Engineering*, 49(5):569–575, 1971. ISSN 1939-019X. doi: 10.1002/cjce.5450490504. URL <http://dx.doi.org/10.1002/cjce.5450490504>.
- P. J. Carreau, M. Devic, and M. Kapellas. Dynamique des bulles en milieu viscoélastique. *Rheologica Acta*, 1974.
- E. Zana and L.G. Leal. The dynamics and dissolution of gas bubbles in a viscoelastic fluid. *International Journal of Multiphase Flow*, 4(3):237 – 262, 1978. ISSN 0301-9322. doi: [http://dx.doi.org/10.1016/0301-9322\(78\)90001-0](http://dx.doi.org/10.1016/0301-9322(78)90001-0).
- Yoshinori Kawase and Jaromir J. Ulbrecht. On the abrupt change of velocity of bubbles rising in non-newtonian liquids. *Journal of Non-Newtonian Fluid Mechanics*, 8(3–4):203 – 212, 1981. ISSN 0377-0257. doi: [http://dx.doi.org/10.1016/0377-0257\(81\)80020-1](http://dx.doi.org/10.1016/0377-0257(81)80020-1).
- D. Dekée, P.J. Carreau, and J. Mordarski. Bubble velocity and coalescence in viscoelastic liquids. *Chemical Engineering Science*, 41(9):2273 – 2283, 1986. ISSN 0009-2509. doi: [http://dx.doi.org/10.1016/0009-2509\(86\)85078-3](http://dx.doi.org/10.1016/0009-2509(86)85078-3).
- S. Gummalam, K.A. Narayan, and R.P. Chhabra. Rise velocity of a swarm of spherical bubbles through a non-newtonian fluid: Effect of zero shear viscosity. *International Journal of Multiphase Flow*, 14(3):361 – 373, 1988. ISSN 0301-9322. doi: [http://dx.doi.org/10.1016/0301-9322\(88\)90050-X](http://dx.doi.org/10.1016/0301-9322(88)90050-X).
- D. De Kee, R.P. Chhabra, and A. Dajan. Motion and coalescence of gas bubbles in non-newtonian polymer solutions. *Journal of Non-Newtonian Fluid Mechanics*, 37(1):1 – 18, 1990. ISSN 0377-0257. doi: [http://dx.doi.org/10.1016/0377-0257\(90\)80001-G](http://dx.doi.org/10.1016/0377-0257(90)80001-G).
- M. Manjunath and R.P. Chhabra. Free rise velocity of a swarm of spherical gas bubbles through a quiescent power law liquid. *International Journal of Engineering Science*, 30(7):871 – 878, 1992. ISSN 0020-7225. doi: [http://dx.doi.org/10.1016/0020-7225\(92\)90016-A](http://dx.doi.org/10.1016/0020-7225(92)90016-A).
- Toshiro Miyahara and Shuichi Yamanaka. Mechanics of motion and deformation of a single bubble rising through quiescent highly viscous newtonian and non-newtonian media. *Journal of Chemical Engineering of Japan*, 26(3):297–302, 1993. doi: 10.1252/jcej.26.297.
- Y. J. Liu, T. Y. Liao, and D. D. Joseph. A two-dimensional cusp at the trailing edge of an air bubble rising in a viscoelastic liquid. *Journal of Fluid Mechanics*, 304:321–342, 12 1995. ISSN 1469-7645. doi: 10.1017/S0022112095004447. URL http://journals.cambridge.org/article_S0022112095004447.

- D. Rodrigue, D. De Kee, and C.F. Chan Man Fong. An experimental study of the effect of surfactants on the free rise velocity of gas bubbles. *Journal of Non-Newtonian Fluid Mechanics*, 66(2):213 – 232, 1996. ISSN 0377-0257. doi: [http://dx.doi.org/10.1016/S0377-0257\(96\)01486-3](http://dx.doi.org/10.1016/S0377-0257(96)01486-3).
- H.Z. Li, Y. Mouline, L. Choplin, and N. Midoux. Chaotic bubble coalescence in non-newtonian fluids. *International Journal of Multiphase Flow*, 23(4):713 – 723, 1997. ISSN 0301-9322. doi: [http://dx.doi.org/10.1016/S0301-9322\(97\)00004-9](http://dx.doi.org/10.1016/S0301-9322(97)00004-9).
- R. P. Chhabra. Rising velocity of a swarm of spherical bubbles in power law fluids at high reynolds numbers. *The Canadian Journal of Chemical Engineering*, 76(1):137–140, 1998. ISSN 1939-019X. doi: 10.1002/cjce.5450760118. URL <http://dx.doi.org/10.1002/cjce.5450760118>.
- Vishal Gauri and W. Kurt Koelling. The motion of long bubbles through viscoelastic fluids in capillary tubes. *Rheologica Acta*, 38(5):458–470, 1998. ISSN 1435-1528. doi: 10.1007/s003970050197. URL <http://dx.doi.org/10.1007/s003970050197>.
- N. Dubash and I.A. Frigaard. Propagation and stopping of air bubbles in carbopol solutions. *Journal of Non-Newtonian Fluid Mechanics*, 142(1):123 – 134, 2007. ISSN 0377-0257. doi: <http://dx.doi.org/10.1016/j.jnnfm.2006.06.006>. URL <http://www.sciencedirect.com/science/article/pii/S0377025706001637>.
- J. Tsamopoulos, Y. Dimakopoulos, N. Chatzidai, G. Karapetsas, and M. Pavlidis. Steady bubble rise and deformation in Newtonian and viscoplastic fluids and conditions for bubble entrapment. *Journal of Fluid Mechanics*, 601:123–164, 2008. doi: 10.1017/S0022112008000517. URL <http://www.scopus.com/inward/record.url?eid=2-s2.0-42449160607&partnerID=40&md5=c188f7b8fcb9c9f30299e32bba9d8c77>.
- Darek Sikorski, Herve Tabuteau, and John R. de Bruyn. Motion and shape of bubbles rising through a yield-stress fluid. *Journal of Non-Newtonian Fluid Mechanics*, 159(1):10 – 16, 2009. ISSN 0377-0257. doi: <http://dx.doi.org/10.1016/j.jnnfm.2008.11.011>. URL <http://www.sciencedirect.com/science/article/pii/S0377025708002140>.
- Nanda Kishore, V. S. Nalajala, and Raj P. Chhabra. Effects of contamination and shear-thinning fluid viscosity on drag behavior of spherical bubbles. *Industrial & Engineering Chemistry Research*, 52(17):6049–6056, 2013. doi: 10.1021/ie4003188.
- Manoj Kumar Tripathi, Kirti Chandra Sahu, George Karapetsas, and Omar K. Matar. Bubble rise dynamics in a viscoplastic material. *Journal of Non-Newtonian Fluid Mechanics*, (0):article in press, 2015. ISSN 0377-0257.
- Amol A. Kulkarni and Jyeshtharaj B. Joshi. Bubble formation and bubble rise velocity in gas-liquid systems: A review. *Industrial & Engineering Chemistry Research*, 44(16):5873–5931, 2005.

- R.P. Chhabra. *Bubbles, Drops, and Particles in Non-Newtonian Fluids*. CRC Press, 2006.
- W. Abbassi, S. Besbes, M. Elhajem, H. Ben Aissia, and J.Y. Champagne. Numerical simulation of free ascension and coaxial coalescence of air bubbles using the volume of fluid method (vof). *Computers & Fluids*, 161:47–59, 2018. ISSN 0045-7930.
- M. Gumulya, R.P. Utikar, G.M. Evans, J.B. Joshi, and V. Pareek. Interaction of bubbles rising inline in quiescent liquid. *Chemical Engineering Science*, 166:1–10, 2017. ISSN 0009-2509.
- Masao Watanabe and Toshiyuki Sanada. In-line motion of a pair of bubbles in a viscous liquid. *Jsme International Journal Series B-fluids and Thermal Engineering*, 49:410–418, 2006.
- H. Yuan and A. Prosperetti. On the in-line motion of two spherical bubbles in a viscous fluid. *Journal of Fluid Mechanics*, 278:325–349, 1994.
- Dominique Legendre, Jacques Magnaudet, and Guillaume Mougin. Hydrodynamic interactions between two spherical bubbles rising side by side in a viscous liquid. *Journal of Fluid Mechanics*, 497:133–166, 2003.
- Zhao Yu, Hui Yang, and Liang-Shih Fan. Numerical simulation of bubble interactions using an adaptive lattice boltzmann method. *Chemical Engineering Science*, 66(14):3441–3451, 2011. ISSN 0009-2509. 10th International Conference on Gas–Liquid and Gas–Liquid–Solid Reactor Engineering.
- J. Katz and C. Meneveau. Wake-induced relative motion of bubbles rising in line. *International Journal of Multiphase Flow*, 22(2):239–258, 1996. ISSN 0301-9322.
- M.C Ruzicka. On bubbles rising in line. *International Journal of Multiphase Flow*, 26(7):1141–1181, 2000. ISSN 0301-9322.
- C. W Hirt and B. D Nichols. Volume of Fluid (VOF) method for the dynamics of free boundaries. *Journal of Computational Physics*, 39(1):201–225, January 1981. ISSN 00219991.
- Murray Rudman. A volume-tracking method for incompressible multifluid flows with large density variations. *International Journal for Numerical Methods in Fluids*, 28(2):357–378, August 1998. ISSN 0271-2091.
- Sharen J. Cummins, Marianne M. Francois, and Douglas B. Kothe. Estimating curvature from volume fractions. *Computers & Structures*, 83(6-7):425 – 434, 2005. ISSN 0045-7949.
- Marianne M. Francois, Sharen J. Cummins, Edward D. Dendy, Douglas B. Kothe, James M. Sicilian, and Matthew W. Williams. A balanced-force algorithm for continuous and sharp interfacial surface tension models within a volume tracking framework. *Journal of Computational Physics*, 213(1):141–173, March 2006. ISSN 00219991.

- Zhaoyuan Wang and Albert Y. Tong. A sharp surface tension modeling method for two-phase incompressible interfacial flows. *International Journal for Numerical Methods in Fluids*, 64(7): 709–732, September 2010. ISSN 02712091.
- Purushotam Kumar, Kai Jin, and S. Pratap Vanka. A multi-GPU based accurate algorithm for simulations of gas-liquid flows. *Computational Methods and Tools in Thermal Fluids Sciences*, pages 1–17, 2015b.
- K. Jin, P. Kumar, S. P. Vanka, and B. G. Thomas. Rise of an argon bubble in liquid steel in the presence of a transverse magnetic field. *Physics of Fluids*, 28(9), 2016. ISSN 10897666. doi: 10.1063/1.4961561.
- William J. Rider and Douglas B. Kothe. Reconstructing volume tracking. *Journal of Computational Physics*, 141(2):112–152, April 1998. ISSN 00219991.
- WF Noh and P Woodward. SLIC (simple line interface calculation). In *Proceedings of the Fifth International Conference*, pages 330–340, Berlin, 1976. Springer-Verlag.
- Jie Li. Calcul d’Interface Affine par Morceaux(piecewise linear interface calculation). *C. R. Acad. Sci. Paris*, 320(8):391–396, 1995.
- N Ashgriz and JY Poo. FLAIR: flux line-segment model for advection and interface reconstruction. *Journal of Computational Physics*, 93(2):449–468, April 1991. ISSN 00219991.
- Yuriko Renardy and Michael Renardy. PROST: a parabolic reconstruction of surface tension for the volume-of-fluid method. *Journal of Computational Physics*, 183(2):400–421, December 2002. ISSN 00219991.
- Mark Sussman. A second order coupled level set and volume-of-fluid method for computing growth and collapse of vapor bubbles. *Journal of Computational Physics*, 187(1):110–136, May 2003. ISSN 00219991.
- M. Sussman, K.M. Smith, M.Y. Hussaini, M. Ohta, and R. Zhi-Wei. A sharp interface method for incompressible two-phase flows. *Journal of Computational Physics*, 221(2):469–505, February 2007. ISSN 00219991.
- Denis Gueyffier, Jie Li, Ali Nadim, Ruben Scardovelli, and Stéphane Zaleski. Volume-of-Fluid interface tracking with smoothed surface stress methods for three-dimensional flows. *Journal of Computational Physics*, 152(2):423–456, July 1999. ISSN 00219991.
- S. P. Vanka, P. Kumar, K. Jin, and B. G. Thomas. Single and multiphase flow computations on graphics processing units. *International Conference on Computational Methods for Thermal Problems*, (217349), 2016. ISSN 2305-5995.

- Purushotam Kumar. *Development and application of Lattice Boltzmann and accurate volume of fluid numerical techniques on graphics processing units*. PhD thesis, University of Illinois at Urbana-Champaign, 2016.
- Jeremy Horwitz, Purushotam Kumar, and Pratap Vanka. Simulations of multiphase flow in a t-junction and distributor header. *Bulletin of the American Physical Society*, 57, 2012.
- Jeremy Horwitz, Purushotam Kumar, and Pratap Vanka. Simulations of three-dimensional droplet deformation in a square-duct at moderate reynolds numbers. *Bulletin of the American Physical Society*, 58, 2013.
- Purushotam Kumar, Jeremy Horwitz, and Surya Vanka. A three-dimensional numerical study of immiscible droplet deformation in a right angle bend. *Bulletin of the American Physical Society*, 58, 2013.
- Purushotam Kumar, Kai Jin, and Surya Pratap Vanka. Numerical Simulation of a Gas Bubble Rising in Power-Law Fluids Using a Sharp Surface Force Implementation. *Proceedings of the ASME-JSME-KSME 2019 8th Joint Fluids Engineering Conference. Volume 5: Multiphase Flow*. San Francisco, California, USA, July 28-August 01, 2019.
- JAK Horwitz, P Kumar, and SP Vanka. Three-dimensional deformation of a spherical droplet in a square duct flow at moderate reynolds numbers. *International journal of multiphase flow*, 67: 10–24, 2014.
- Jeremy A. K. Horwitz, S. P. Vanka, and P. Kumar. Lbm simulations of dispersed multiphase flows in a channel: Role of a pressure poisson equation. *Proceedings of the ASME-JSME-KSME 2019 8th Joint Fluids Engineering Conference. Volume 5: Multiphase Flow*. San Francisco, California, USA, July 28-August 01, 2019.
- Surya Pratap Vanka, Kai Jin, Purushotam Kumar, and Brian Thomas. Rise of an argon bubble in liquid steel in the presence of a transverse magnetic field. *Bulletin of the American Physical Society*, 60, 2015.
- Purushotam Kumar and Pratap Vanka. Dynamics of Argon Gas Bubble Pair Rising in Liquid Steel in the Presence of a Transverse Magnetic Field. *Bulletin of the American Physical Society*, 67, 2022.
- Purushotam Kumar and Surya Pratap Vanka. Dynamics of argon gas bubbles rising in liquid steel in the presence of transverse magnetic field. *arXiv preprint arXiv:2301.01797*, 2023.
- Pratap Vanka, Purushotam Kumar, and Kai Jin. Numerical Simulation of Turbulent Bubbly Flow in a Vertical Square Duct. *Bulletin of the American Physical Society*, 61, 2016.

- Purushotam Kumar and Surya Pratap Vanka. Large scale gpu based simulations of turbulent bubbly flow in a square duct. *arXiv preprint arXiv:2104.01636*, 2021.
- Mitsuhiro Ohta, Eiji Iwasaki, Eiji Obata, and Yutaka Yoshida. A numerical study of the motion of a spherical drop rising in shear-thinning fluid systems. *Journal of Non-Newtonian Fluid Mechanics*, 116(1):95 – 111, 2003. ISSN 0377-0257. doi: <http://dx.doi.org/10.1016/j.jnnfm.2003.08.004>.
- Li Zhang, Chao Yang, and Zai-Sha Mao. Numerical simulation of a bubble rising in shear-thinning fluids. *Journal of Non-Newtonian Fluid Mechanics*, 165(11-12):555 – 567, 2010. ISSN 0377-0257. doi: <http://dx.doi.org/10.1016/j.jnnfm.2010.02.012>.
- Mitsuhiro Ohta, Sachika Kimura, Tomohiro Furukawa, Yutaka Yoshida, and Mark Sussman. Numerical simulations of a bubble rising through a shear-thickening fluid. *Journal of Chemical Engineering of Japan*, 45(9):713–720, 2012. doi: 10.1252/jcej.12we041.
- Pierre J. Carreau. Rheological equations from molecular network theories. *Transactions of The Society of Rheology*, 16(1), 1972.